

## 1 Neutron stars

A neutron star is formed from the remnant of a supernova, leaving a 1.3 to perhaps 2.1 solar mass in the collapse. A typical radius is about 10 km producing approximately 10 times nuclear density in its interior. The nuclear equation of state can only be theoretically estimated, but calculations indicate that hyperons appear as constituents at about twice nuclear density and can become significant components at about 4 time nuclear densities. More recently, the observation that the  $\Sigma^-$ -nucleus potential is repulsive has led to the re-organization of the list of hyperon components with the  $\Xi^-$  replacing the  $\Sigma^-$  constituents. The component population is sensitive to the in-medium potentials, and of course there is no experimental hyperon-hyperon data.

The introduction of hyperons into a neutron star affects the maximum mass of the star. Without hyperons and a soft equation of state, the maximum mass is approximately 2.4 solar masses. With hyperons the maximum mass can apparently be no larger than 1.7 solar masses. However, a recently identified neutron star appears to have a mass of about 2.1 solar masses. Perhaps the equation of state is too soft and/or hyperon-hyperon interactions are not properly included. However, it is also possible that a star having a mixed phase of hyperons and quarks in its interior is produced. Because the star rapidly rotates, losing energy via radiation, the rotational inertia of the star changes, and the rotational frequency depends on its composition which is coupled to the rotational frequency. Obviously more astrophysical observations are needed, however the only terrestrial handle on this physics comes from hypernuclei, particularly multi-strange hypernuclei.

Although neutron star composition at low density is dominated by neutrons, transmutation to hyperons, beginning at 2 to 3 times normal nuclear matter density  $\rho_0 = 0.17 \text{ fm}^{-3}$ , would act to alleviate the Pauli pressure of nucleons and leptons. Matter in the core of neutron stars can be further compressed to about  $(5 - 6)\rho_0$ . At these densities strange hadronic matter, which may already be self bound at densities  $(2 - 3)\rho_0$ , could become stable even to weak decay. Such matter may perhaps form kaon condensates and even deconfine to quarks, forming strange quark matter.

## 2 Strange hadronic matter

Strange quark matter, with roughly equal composition of  $u$ ,  $d$  and  $s$  quarks, might provide an absolutely stable form of matter. Finite strange quark systems, so called strangelets, have

also been considered.

Less known is the more recent observation that metastable strange systems with similar properties, i.e. a strangeness fraction  $f_S \equiv -S/A \approx 1$  and a charge fraction  $f_Q \equiv Z/A \approx 0$ , might also exist in hadronic form at moderate values of density between twice and three times nuclear matter density. These strange systems are made of  $N$ ,  $\Lambda$  and  $\Xi$  baryons. The metastability (i.e. stability with respect to strong interactions, but not to  $\Delta S \neq 0$  weak-interaction decays) of these strange hadronic systems was established by extending relativistic mean field (RMF) calculations from ordinary nuclei ( $f_S = 0$ ) to multi-strange nuclei with  $f_S \neq 0$ . Although the detailed pattern of metastability, as well as the actual values of the binding energy, depend specifically on the incompletely known hyperon potentials in dense matter. A conservative example is given in Fig. 2, assuming a relatively weak hyperon-hyperon attractive interaction. The figure shows the calculated binding energy of  $^{56}\text{Ni} + N_\Lambda \Lambda$  multi- $\Lambda$  hypernuclei for  $N_\Lambda = 0, 2, 8, 14$  and how it becomes energetically favorable to add  $\Xi$  hyperons when  $N_\Lambda$  exceeds some fairly small threshold value. As soon as the  $\Lambda$   $p$ -shell is filled,  $\Xi$  hyperons may be placed in their  $s$ -shell owing to Pauli blocking of the strong-interaction conversion process  $\Xi N \rightarrow \Lambda \Lambda$  which in free space releases about 25 MeV.

In other calculations, it was found that strange hadronic matter (SHM) is comfortably metastable for any allowed value of  $f_S > 0$ . However for  $f_S \geq 1$ ,  $\Sigma$ s replace  $\Lambda$ s due to the exceptionally strong  $\Sigma\Sigma$  and  $\Sigma\Xi$  interactions in this model. A first-order phase transition occurs from  $N\Lambda\Xi$  dominated matter for  $f_S \leq 1$  to  $N\Sigma\Xi$  dominated matter for  $f_S \geq 1$ , as shown in Fig. 3 where the binding energy versus the baryon density is shown for several representative values of  $f_S$ . At  $f_S \approx 1.0$  a secondary minimum at higher baryon density becomes energetically favored. The system then undergoes a first-order phase transition from the low density state to the high density state.

Fig. 4 demonstrates explicitly that the phase transition involves transformation from  $N\Lambda\Xi$  dominated matter to  $N\Sigma\Xi$  dominated matter, by showing the calculated composition of SHM for this model (denoted N for Nijmegen) as function of the strangeness fraction  $f_S$ . The particle fractions for each baryon species change as function of  $f_S$ . At  $f_S = 0$ , one has pure nuclear matter, whereas at  $f_S = 2$  one has pure  $\Xi$  matter. In between, matter is composed of baryons as dictated by chemical equilibrium. A change in the particle fraction may occur quite drastically when new particles appear, or existing ones disappear. A sudden change in the composition is seen in Fig. 4 for  $f_S = 0.2$  when  $\Xi$ s (long-dashed line) emerge in the medium, or at  $f_S = 1.45$  when nucleons (short-dashed line) disappear. The situation at  $f_S = 0.95$  is a special one, as  $\Sigma$ s (solid line) appear in the medium, marking the first-order phase transition observed in the previous figure. The baryon composition alters completely at that point, from  $N\Xi$  baryons plus a rapidly vanishing fraction of  $\Lambda$ s (dot-dashed line) into  $\Sigma\Xi$  hyperons plus a decreasing fraction of nucleons. At the very deep minimum of the binding energy curve (not shown here) SHM is composed mainly of  $\Sigma$ s and  $\Xi$ s with a very small admixture of nucleons. Unfortunately, it will be difficult to devise an experiment to

determine the depth of the  $\Lambda\xi$ ,  $\Xi\xi$ ,  $\Xi\Sigma$ ,  $\Sigma\Sigma$  interaction potentials, which are so crucial to verify these results.

### 3 Summary

As a function of density, the first hyperon to appear is the lightest one, the  $\Lambda$  at about  $2\rho_0$ , by converting protons and electrons directly to  $\Lambda$ s instead of neutrons, thereby decreasing the neutron Pauli pressure. It is reasonable to assume that this composition varies radially, perhaps having a crust and an atmosphere composed of neutrons. Among the negatively charged hyperons the lightest one,  $\Sigma^-$ , does not appear at all over the wide range of densities shown owing to its repulsion in nuclear matter, and most likely also in neutron matter. Its potential role in reducing the Pauli pressure of the leptons ( $e^-$  and  $\mu^-$ ) could be replaced by the heavier  $\Xi^-$  hyperon, assuming overall  $\Xi$ -nuclear attraction. The specific calculation sketched by Fig. 5 predicts that the hyperon population takes over the nucleon population for densities larger than about  $6\rho_0$ , where the inner core of a neutron star may be viewed as a giant hypernucleus.

Given the high matter density expected in a neutron star, a phase transition from ordinary nuclear matter to some exotic mixtures cannot be ruled out. Whether a stable star is composed dominantly of hyperons, quarks, or some mixture thereof, and just how this occurs, is not clear as both the strong and weak interactions, which operate on inherently different time scales, are in play. The equation of state (EoS) of any possible composition constrains the mass-radius ( $M - R$ ) relationship for a rotating neutron star. Thus, the maximum mass  $M_{\max}$  for a relativistic free neutron gas is given by  $M_{\max} \approx 0.7M_\odot$ , whereas higher mass limits are obtained under more realistic EoS assumptions. Without strangeness, but for interacting nucleons (plus leptons)  $M_{\max}$  comes out invariably above  $2M_\odot$ , as shown by the curves marked *n-matter* and *ChEFT* in Fig. 6. Allowing for strangeness through hyperons softens the EoS, thereby lowering  $M_{\max}$  to the range  $(1.4 - 1.8)M_\odot$ , also if/when a phase transition occurs to strange hadronic matter. Considerably lower values of  $M_{\max}$ , below  $M_\odot$ , are reached for purely two-body interactions as shown by the  $\Lambda N$  red curve in Fig. 6 taken from a recent Quantum Monte Carlo (QMC) calculation of  $\Lambda$  hypernuclei. The effect of kaon condensation, delayed by hyperons, is to lower  $M_{\max}$  further by just a tiny  $\approx 0.01M_\odot$ .  $M_{\max}$  values of up to  $2M_\odot$  are within the reach of hybrid (nuclear plus quark matter) star calculations in which strangeness materializes via non-hadronic degrees of freedom.

Until recently, the neutron star mass distribution for radio binary pulsars was given by a narrow Gaussian with mean & width values  $(1.35 \pm 0.04)M_\odot$ , somewhat below the Chandrasekhar limit of  $1.4M_\odot$  for white dwarfs, above which these objects become gravitationally unstable. However, there is now some good evidence from X-ray binaries classified as neutron stars for masses about and greater than  $2M_\odot$ . The highest *accepted* value of neutron star mass is provided at present by the precise mass measurements of the pulsars

PSR J1614-2230 and PSR J0348+0432 , marked by horizontal lines in Fig. 6. These yield nearly  $2M_{\odot}$  and thereby exclude several ‘soft’ EoS scenarios for dense matter . The figure demonstrates how the gradual introduction of repulsive  $\Lambda NN$  interactions , from version 1 to version 2, leads to a corresponding increase of the calculated  $M_{\max}$  value by increasing the matter density  $\rho_{\min}$  at which  $\Lambda$  hyperons appear first in neutron matter to higher values, until this  $\rho_{\min}$  exceeds the value  $\rho_{\max}$  corresponding to  $M_{\max}$ . When this happens, for version 2, the mass-radius dotted curve overlaps with the purely ‘ $n$ -matter’ green curve below the point marked in the figure for the value of  $M_{\max}$  reached. This scenario of including strongly repulsive  $\Lambda NN$  forces may prove instrumental in resolving the ‘hyperon puzzle’, by explaining why and how hyperons are excluded from the EoS of neutron stars. Fig. 7 shows how the introduction of these repulsive  $\Lambda NN$  interactions within QMC calculations relieves the over-binding of  $\Lambda$  hypernuclei which arises progressively with increasing the mass number  $A$  (corresponding to smaller values of  $A^{-2/3}$  in the figure) upon using microscopically constructed purely two-body  $\Lambda N$  interactions dominated by attraction. In particular, the same version ‘ $\Lambda N + \Lambda NN$  (II)’ that according to Fig. 6 resolves the ‘hyperon puzzle’, according to Fig. 7 also resolves the ‘ $B_{\Lambda}$  over-binding’ problem. More work is required in this direction, say by introducing  $\Xi^{-}$  hyperons, to make sure that the ‘hyperon puzzle’ has indeed been resolved in this way.

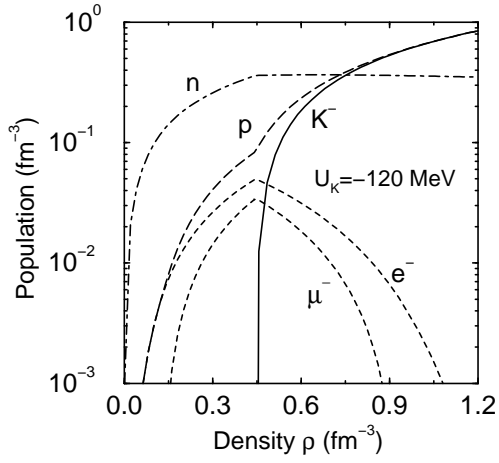


Figure 1: Population of neutron star matter, allowing for kaon condensation, calculated as a function of nucleon density.

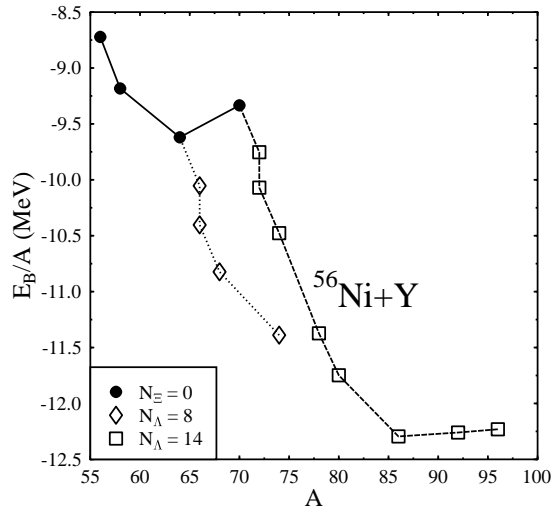


Figure 2: Calculated binding energy of multistrange nuclei of  $^{56}\text{Ni}$  plus  $\Lambda$  and  $\Xi$  hyperons, as function of baryon number  $A$ .

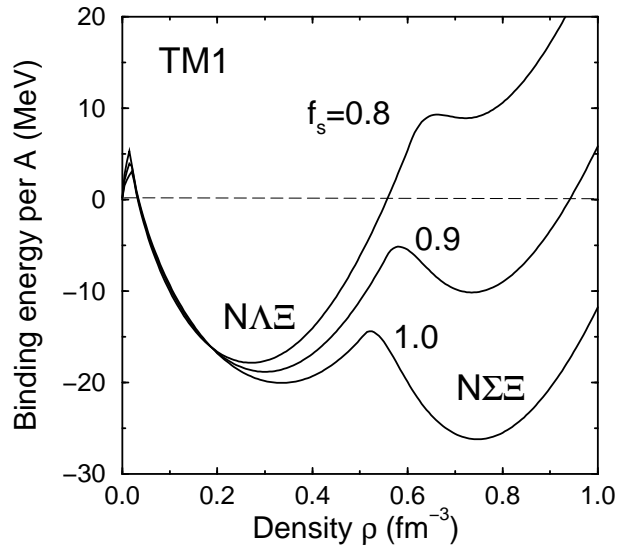


Figure 3: Transition from  $N\Lambda\Xi$  to  $N\Sigma\Xi$  matter upon increasing the strangeness fraction.

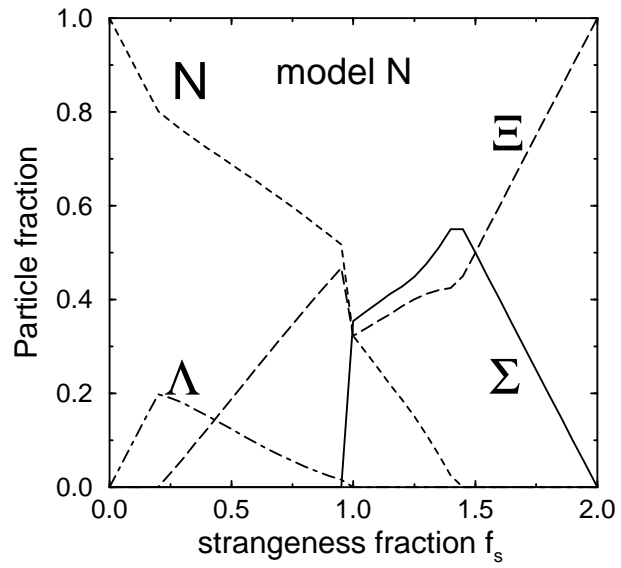


Figure 4: Strange hadronic matter composition as function of strangeness fraction  $f_S$ .

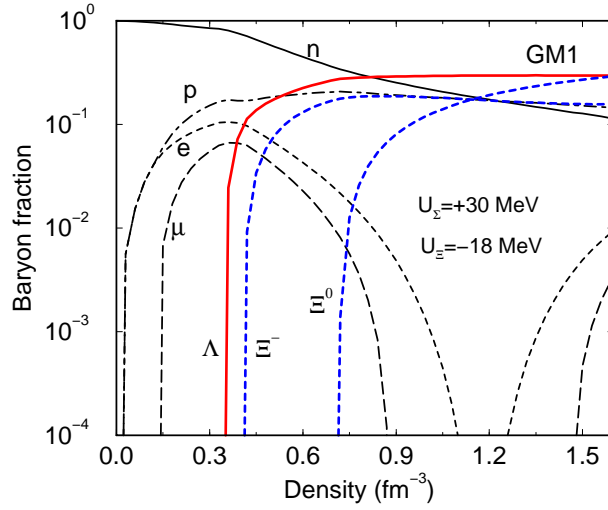


Figure 5: Neutron star matter fractions of baryons and leptons, calculated as a function of density.

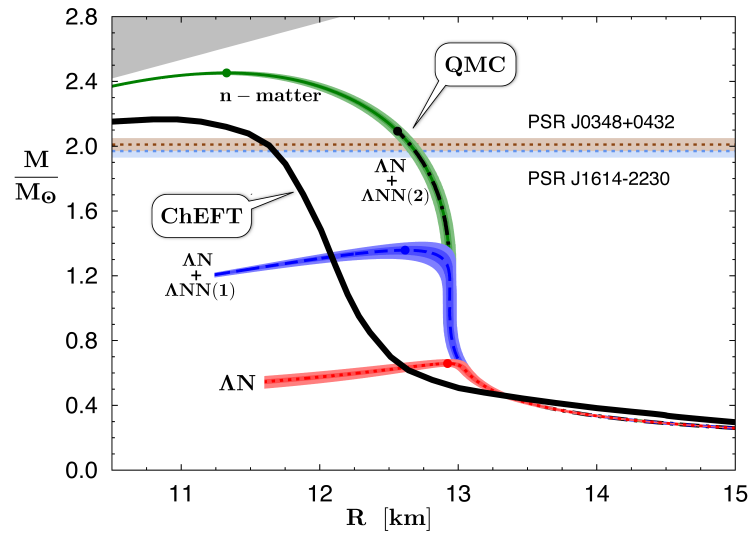


Figure 6: Mass-radius relationship for various EoS scenarios of neutron stars, including nucleons and leptons only as well as upon including  $\Lambda$  hyperons.

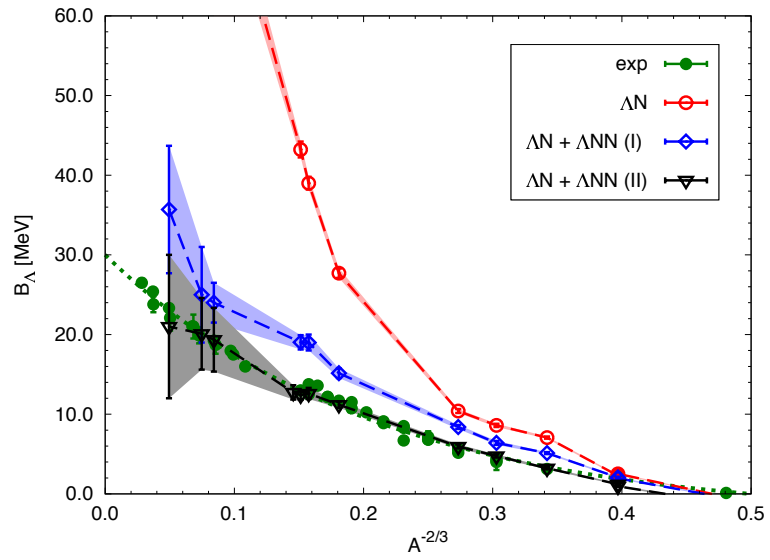


Figure 7: QMC calculations of  $\Lambda$  hypernuclear binding energies for purely two-body  $\Lambda N$  interactions and for two versions of adding repulsive  $\Lambda NN$  interactions. Figure adapted from .